On the Reorientation and Hydrogen-Bond Dynamics of Alcohols

Anthony A. Vartia,[†] Katie R. Mitchell-Koch,[†,§] Guillaume Stirnemann,[‡] Damien Laage,[‡] and Ward H. Thompson[*,†]

[†]Department of Chemistry, University of Kansas, Lawrence, Kansas 66045, United States
[‡]Department of Chemistry, Ecole Normale Supérieure, UMR ENS-CNRS-UPMC 8640, 24 rue Lhomond, 75005 Paris, France

ABSTRACT: The mechanism of the OH bond reorientation in liquid methanol and ethanol is examined. It is found that the extended jump model, recently developed for water, describes the OH reorientation in these liquids. The slower reorientational dynamics in these alcohols compared to water can be explained by two key factors. The alkyl groups on the alcohol molecules exclude potential partners for hydrogen bonding exchanges, an effect that grows with the size of the alkyl chain. This increases the importance of the reorientation of intact hydrogen bonds, which also slows with increasing size of the alcohol and becomes the dominant reorientation pathway.
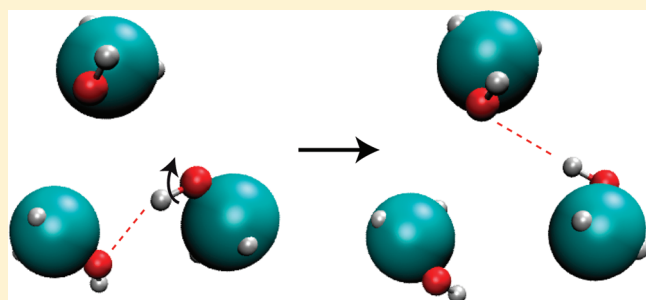
1. INTRODUCTION

Reorientational dynamics in liquids play a critical role in numerous chemical phenomena ranging from charge transfer reactions to dielectric response. Thus, it is useful to understand the mechanisms and time scales of molecular rotation, particularly how these change between different liquids. Alcohols are an important case in this context as they are used in many applications as solvents and, together with water, they offer a series over which trends can be examined. While, compared to water, there is limited experimental data on the reorientational dynamics of liquid alcohols, from those results it is clear that the OH-bond reorientation slows with increasing length of the alkyl group of the alcohol.[1−6] In this paper, we focus on the more studied,[1−31] smallest alcohols, methanol and ethanol, and investigate the origin of these slower dynamics.

The reorientational dynamics can be characterized by the autocorrelation functions

$$C_\ell(t) = \langle P_\ell[\mathbf{e}(t) \cdot \mathbf{e}(0)] \rangle \tag{1}$$

where $\mathbf{e}$ is the unit vector along a particular molecular axis, P_ℓ is the ℓth Legendre polynomial, and $\langle \cdot \rangle$ indicates a thermal average. These correlation functions measure the time scales for reorientation of the molecules in the liquid. In this paper, we will consider only the case where $\mathbf{e}$ is along the OH bond and $\ell = 2$, that is, $C_2(t)$ for OH reorientation. This correlation function is accessible in infrared pump−probe anisotropy measurements, as well as NMR experiments. In the former, the correlation function is directly accessed, and we will focus on the longest time scale in the decay of $C_2(t)$, denoted as τ_2. In NMR measurements, the average time

$$\langle \tau \rangle = \int_0^\infty C_2(t) dt \tag{2}$$

is obtained.

The $C_2(t)$ correlation functions for liquid water, methanol, and ethanol, calculated from MD simulations, are shown in Figure 1. The decay of $C_2(t)$ occurs on multiple time scales. For the present purposes these have been obtained by a triexponential fitting of $C_2(t)$; we have verified that the longest time scales, which are the focus here, are only slightly affected by the choice of fitting procedure. This yields $\tau_2 = 2.6 \pm 0.1$, 5.5 ± 0.3, and 12.1 ± 1.7 ps for water, methanol, and ethanol, respectively. These yield average integrated decay times of $\langle \tau \rangle = 1.7 \pm 0.1$, 3.3 ± 0.3, and 6.3 ± 1.8 ps for the three liquids. The simulations thus reproduce, with some quantitative differences,[32] the trend previously derived from NMR measurements that yielded $\langle \tau \rangle = 1.7 - 2.6$ for water,[33−35] 5 ps for methanol,[1−3] and 12.7 and 18 ps for ethanol.[4,6]

What is the explanation for this trend in the OH reorientational time? Water reorientation has been studied extensively and a detailed picture has been developed.[36,37] The central element of the mechanism for reorientation is the hydrogen bond exchange, or "jump," dynamics. That is, the picture is that the OH bonds reorient primarily through switching hydrogen bonding partners, with a more minor contribution of the overall, "frame," reorientation of the intact hydrogen bond itself between jumps. This is expressed mathematically within the extended jump model (EJM) of Laage and Hynes.[36,37] It is then plausible to suppose that the OH bonds in simple alcohols like methanol and ethanol reorient by a similar hydrogen bond jump mechanism. The slower reorientational times might then be due to differences in the nature of these jumps or the barriers involved. However, additional insight is provided by a recent study of water reorientational dynamics around hydrophobic solutes by Laage et al.[38]
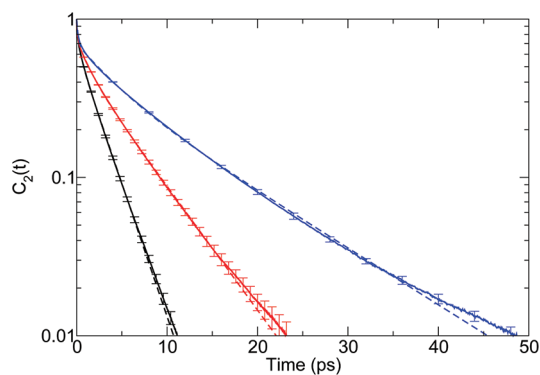
Figure 1. Reorientational correlation function, $C_2(t)$, is plotted versus time for water (black line), methanol (red line), and ethanol (blue line). Dashed lines represent the multiexponential fits (see the text).

Figure 2. Jump angle distributions for hydrogen bond switches in water (black), methanol (red), and ethanol (blue).

It was found that the slowdown in water reorientation around such solutes could be attributed to the excluded volume of the solutes. Effectively, the solutes limit the space available around an adjacent water molecule in which a new hydrogen bonding partner can be found, slowing the hydrogen bond exchange dynamics.

The extension of this idea to the simple alcohols then suggests that reorientation of the OH bonds in alcohols is slowed due to the excluded volume of the alkyl group. In the following, we use MD simulations together with the EJM to determine the origin of the slowdown in the alcohol reorientation dynamics and assess the impact of the excluded volume contribution.

2. EXTENDED JUMP MODEL (EJM)

We now consider how the EJM can describe the trend in reorientational dynamics. The model combines the reorientational contribution of the jumps between hydrogen-bonding partners with the frame reorientation, that is, that of the $O\cdots O$ vector in an intact hydrogen bond, to describe the $C_2(t)$ reorientation time, τ_2 [37]

$$\frac{1}{\tau_2} = \frac{1}{\tau_2^{\text{jump}}} + \frac{1}{\tau_2^{\text{frame}}} \tag{3}$$

In applying the EJM to understand the differences between water, methanol, and ethanol, we first consider the jump time contribution, τ_2^{jump}, before turning attention to the frame reorientation time component, τ_2^{frame}. The jump time associated with hydrogen-bond switches will be denoted as τ_0 and the contribution to the $C_2(t)$ correlation function, τ_2^{jump}, is then related to τ_0 and the jump angle, $\Delta\theta$

$$\tau_2^{\text{jump}} = \tau_0 \left[1 - \frac{\sin(5\Delta\theta/2)}{5\sin(\Delta\theta/2)} \right]^{-1} \tag{4}$$

Both τ_0 and $\Delta\theta$ can be extracted from the MD simulation data.

The jump angle, $\Delta\theta$, is defined as the $O_A - O_D - O_B$ angle at the transition state of a hydrogen bond exchange. Here, O_D is the oxygen of the OH group that is the hydrogen-bond donor, O_A is the original acceptor, and O_B is the new acceptor after the jump. The jump angle distributions [39] for water, methanol, and ethanol are shown in Figure 2. We first note that the distribution of jump angles for water is in good agreement with that obtained
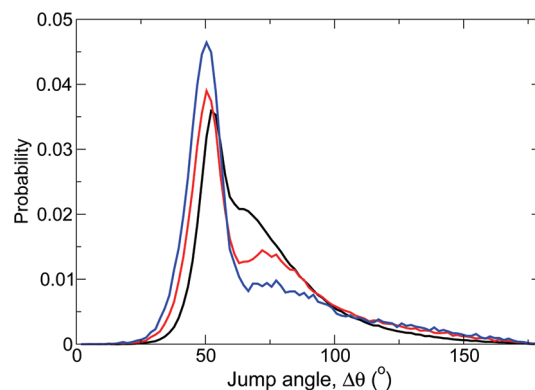
previously.[37] The distribution is peaked at $\theta_{\text{max}} = 52°$ and gives an average jump angle

$$\langle\Delta\theta\rangle = \int_0^\pi P(\Delta\theta)\sin(\Delta\theta)d\Delta\theta \tag{5}$$

of 71°; these compare well to values of $\theta_{\text{max}} = 50°$ and $\langle\Delta\theta\rangle = 68°$ found in ref 37. The distributions for methanol and ethanol differ in two respects: the peak at larger jump angles ($\sim 75°$) is reduced in magnitude from water to methanol to ethanol and this is accompanied by an increase in magnitude and shift of the main peak to slightly smaller jump angles. For methanol (ethanol), the average jump angle is 71° (68°), and the distribution peaks at 50° (50°). (In the following, we use the average jump angles in eq 4 to obtain τ_2^{jump}.) As a whole, these jump angle distributions indicate that there is not a dramatic change in hydrogen bond exchange geometries for the alcohols compared to water. The key difference occurs at larger jump angles and, as will be shown below, can be attributed to the excluded volume of the alkyl group of the donor alcohol molecule.

3. HYDROGEN BOND JUMP TIMES

Having established that the alcohols do not differ significantly from water in the size or distributions of jump angles, $\Delta\theta$, and hence that this cannot explain the differences in reorientation times, we next examine whether the slowdown is due to differences in the time for a hydrogen-bond switch (jump) to occur. The jump time, τ_0, can be calculated from MD simulations in multiple ways. One approach is based on the stable-states picture, which provides the time for switches between hydrogen-bonding partners from the properties of the side−side time-correlation function

$$C_{AB}(t) = \langle n_A(0)n_B(t)\rangle \tag{6}$$

Here, $n_A(0)$ is the population of a hydrogen-bonded state with acceptor O_A at time $t = 0$ and $n_B(t)$ is the population of a hydrogen-bonded state with a different acceptor O_B at a later time t. For a given OH group engaged in a hydrogen bond at time $t = 0$, $n_A(0) = 1$ and A is the identity of the acceptor. Then, $n_B(t)$, and hence the contribution to $C_{AB}(t)$, is zero until the OH group switches into a hydrogen bond with a new acceptor, B, after which $n_B(t) = 1$ and the OH group gives a nonzero contribution to $C_{AB}(t)$. Clearly, this correlation function increases in time with the switching of hydrogen-bonding partners. Absorbing boundary conditions are used so that the correlation function only
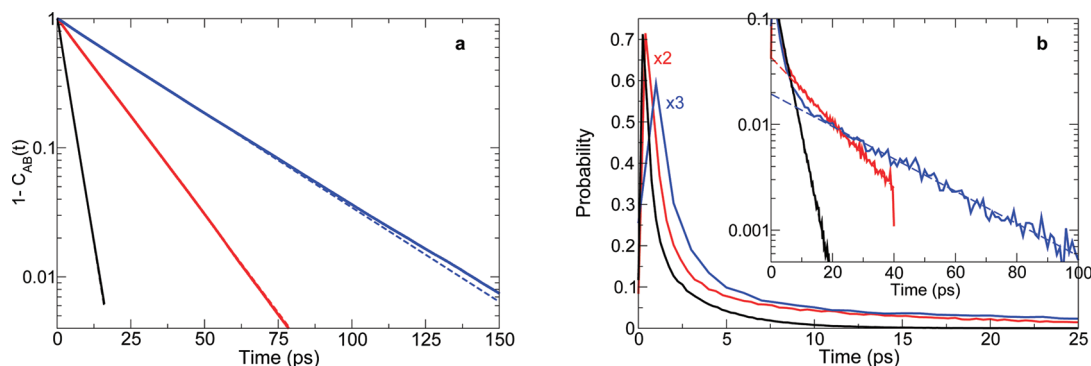
Figure 3. (a) The correlation function $1 - C_{AB}(t)$ is plotted as a function of time for water (black), methanol (red), and ethanol (blue). Single exponential fits are shown as dashed lines of the same color. (b) The waiting-time distribution for hydrogen bonds are shown for water (black), methanol (red), and ethanol (blue). Inset: Long-time decay is shown with single-exponential fits (dashed lines) to the distributions for $t > 5$, 10, and 20 ps for water, methanol, and ethanol, respectively.

Table 1. Reorientational Times, τ_2, for the Water, Methanol, and Ethanol Are Compared with Calculated Jump Times, τ_0, the Jump-Time Contribution to the $C_2(t)$ Reorientational Correlation Function, τ_2^{jump}, and the Corresponding Frame Reorientation Times, τ_2^{frame} [a]

liquid	τ_2	τ_0 SSP[b]	τ_0 WTD[c]	τ_2^{jump} SSP[b]	τ_2^{jump} WTD[c]	τ_2^{frame}
H_2O	2.6 ± 0.1	3.1	3.1	3.2	3.2	5.6
CH_3OH	5.5 ± 0.3	14.3	14.1	14.5	14.3	7.3
C_2H_5OH	12.1 ± 1.7	29.7	28.4	31.7	30.3	15.5

[a] Data is for 298 K and all times are in ps. [b] Obtained from the decay of the stable-states picture correlation function $1 - C_{AB}(t)$. [c] Obtained from the long-time decay of the hydrogen-bond waiting time distribution.

reflects the dynamics of a single jump. Hence, $1 - C_{AB}(t)$ decays in time with a time scale corresponding to the rate constant for hydrogen bond switches, or jumps. Specifically, the jump time can be extracted from this correlation function by fitting to the form $1 - C_{AB}(t) = \exp(-t/\tau_0)$.

The correlation functions $C_{AB}(t)$ obtained for water, methanol, and ethanol are shown in Figure 3a along with their fits to this exponential form. They are well-described by the exponential fits for all cases, with only slight deviations for ethanol at times greater than ~100 ps. The jump times obtained from this fitting are $\tau_0 = 3.1$, 14.3, and 29.7 ps for water, methanol, and ethanol, respectively; see Table 1. The value for water is in good agreement with the 3.3 ps reported previously by Laage and Hynes.[37] The jump time for methanol is more than 4 times longer than that for water and the jumps for ethanol are yet another factor of 2 slower than methanol.

The jump time can also be extracted from the waiting time distribution for hydrogen-bond switches, that is, a histogram of the time for a currently hydrogen-bonded OH group to switch hydrogen-bonding partners. This distribution is shown in Figure 3b for the three liquids. The long-time behavior of this distribution exhibits an exponential decay, the time constant of which can be identified as the jump time τ_0. Fitting this decay gives $\tau_0 = 3.1$, 14.1, and 28.4 ps for water, methanol, and ethanol, respectively, in excellent agreement with the $C_{AB}(t)$ correlation function results.

These data indicate that the slower OH reorientation is partly due to a strong slowdown in the hydrogen-bond jump times.

However, this slowdown might be due to enthalpic or entropic factors, the former attributable to differences in hydrogen bond strengths and the latter related to the available volume for hydrogen-bond switches. The first can be examined through the temperature dependence of τ_2^{-1} which provides the activation energies. The reorientation time displays Arrhenius behavior over the temperature range $T = 280-360$ K as shown in Figure 4. The activation energy for water is 3.50 ± 0.07 kcal/mol, the same as previously obtained[37] under slightly different simulation conditions,[40] close to that obtained for methanol (3.10 ± 0.09 kcal/mol) and, within error bars, the same as that for ethanol (3.73 ± 0.59 kcal/mol). The activation energies for the three liquids are thus approximately the same and the (small) differences do not correlate with slower reorientation for methanol than water. This points to an entropic origin for the slowdown in reorientation.

4. EXCLUDED VOLUME EFFECTS

Focusing on the entropic effects, the slowdown in the reorientational jump times can then be expressed by the ratio of τ_2^{jump}, obtained from eq 4, for the alcohols to that for water. Moreover, in the case of hydrophobic solutes, this was previously[38] related to the excluded volume fraction, f

$$\frac{\tau_2^{jump}(ROH)}{\tau_2^{jump}(H_2O)} = \frac{1}{1-f} \qquad (7)$$

Here, f is the fraction of the volume at the hydrogen-bond jump transition state geometry blocked by atoms, which cannot serve as new acceptors (e.g., CH_2, CH_3). As is discussed in ref 38 and below, f can be calculated directly with some knowledge of the geometry of the transition state for the hydrogen-bond exchanges. However, it can also be obtained from the τ_2^{jump} values just determined. The slowdown factors from eq 7 are large, factors of 4.5 and 10 for methanol and ethanol, giving large excluded volume fractions of $f = 0.78$ and 0.90, respectively. That these values are significantly greater than found previously for dilute hydrophobic solutes should not be a surprise. Every liquid molecule in an alcohol has a hydrophobic component, whereas for hydrophobic or amphiphilic solutes the excluded volume is only external to the reorienting molecules and concentration-dependent; thus, such large values of f are only found at high concentration (e.g., ~6−8 m).[41]
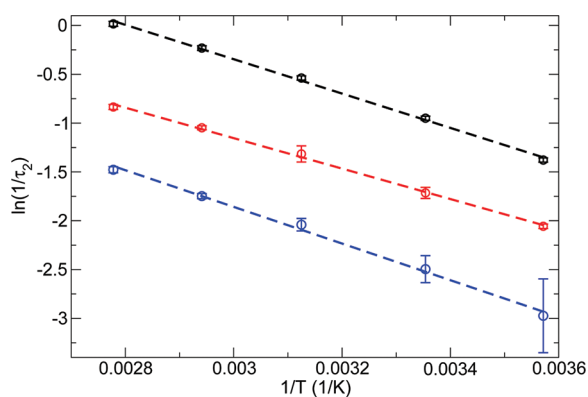
Figure 4. Arrhenius plot for the reorientation time, τ_2, for water (black), methanol (red), and ethanol (blue). Dashed lines represent linear fits; the corresponding activation energies are $E_a = 3.50 \pm 0.07$, 3.10 ± 0.09, and 3.73 ± 0.59 kcal/mol for H_2O, CH_3OH, and C_2H_5OH, respectively.

Table 2. Slowdown Factors for the Reorientational and Jump Times Are Given for Methanol and Ethanol along with Excluded Volume Fractions, f, Estimated from the Slowdown Factors Using eq 7, f_{est}, and Calculated from MD Simulations, f_{calc}

liquid	$\tau_2/\tau_2(H_2O)$	$\tau_2^{jump}/\tau_2^{jump}$ $(H_2O)^a$	f_{est}	$f_{calc}(\langle\Delta\theta\rangle)$	$\langle f_{calc}\rangle$
CH_3OH	2.1	4.5 (4.5)	0.78	0.77	0.78
C_2H_5OH	4.7	10.1 (9.6)	0.90	0.80	0.83

^{a} Obtained from the decay of the stable-states picture correlation function $1 - C_{AB}(t)$; value from the waiting time distribution given in parentheses.

The excluded volume fraction at the transition state geometry can be obtained directly by analysis of the MD simulation trajectories according to the procedure described by Laage et al.[38] Briefly, for each established hydrogen bond, a ring of points is constructed at the location of potential hydrogen bond switch transition states. These are defined by an $O_D \cdots O_B$ distance at the transition state, here taken to be the value of $R^{\ddagger} = 3.5$ Å found for water in ref 37, and the jump angle, $\Delta\theta$. The excluded volume fraction, f, is calculated as the number of the points on this ring falling within the Lennard-Jones radius of any atom that is not a potential new hydrogen-bond acceptor, that is, not O_B. Estimations of the excluded volume fraction for both cases can be found in Table 2.

In the simplest approach, f can be calculated in this way using the average jump angle, $\langle\Delta\theta\rangle$, which is 71° for water and methanol and 68° for ethanol. The value of 0.77 for methanol is in excellent agreement with that obtained directly from the jump times of methanol and water (0.78). The fraction obtained for ethanol, $f(\Delta\theta) = 0.80$, is larger than that for methanol, but only slightly so. A more precise value of f can be obtained by convoluting the excluded volume fraction as a function of jump angle, $f(\Delta\theta)$, and calculating its average, weighted with the jump angle probability distribution

$$\langle f\rangle = \int_0^{\pi} f(\Delta\theta)P(\Delta\theta)\sin(\Delta\theta)d\Delta\theta \qquad (8)$$

The result for methanol, $\langle f\rangle = 0.79$, is nearly the same as that obtained using the average jump angle and that estimated from the slowdown factor for the jump times. The $\langle f\rangle = 0.83$ for ethanol is larger than $f(\langle\Delta\theta\rangle)$ and, given the approximate nature of the estimate,[42] is in good agreement with the value of 0.90 obtained from the jump times.

The contributions to the excluded volume fraction at different jump angles can provide insight into how the hydrogen bond jump dynamics is slowed down in the alcohols. These are presented for methanol and ethanol in Figure 5. As is the case for water,[37] the volume is nearly completely excluded at small jump angles by the hydrogen-bond acceptor molecule itself, leading to a lack of viable jump angles below ∼40°. In methanol and ethanol, the probabilities of larger jump angles (>70°), are diminished compared to water, as seen in Figure 2. The origin of this is clear

from $f(\Delta\theta)$ and its decomposition into specific components. The alkyl groups on the donor molecule itself exclude volume at larger jump angles, $\Delta\theta$ more than ∼70°. The decomposition of $f(\Delta\theta)$ shows that the ethanol CH_2 group on the hydrogen-bond donor has nearly the same effect as the methanol CH_3 group. The additional methyl group in ethanol gives an overall greater excluded volume for that liquid compared to methanol. Thus, steric bulk on the hydrogen-bond donor molecule itself plays a significant role in slowing down hydrogen-bond switching by crowding out potential new acceptors. Finally, it is interesting to note that the excluded volume due to molecules aside from the donor and acceptor is slightly greater in methanol than ethanol. This is more than compensated for by the donor and acceptor, whose volume is presumably also to blame for this effect.

It is instructive to examine whether the longer jump times in the alcohols due to the substantial excluded volume indicates a change in the mechanism from a direct jump between hydrogen-bonding partners to a jump involving an intermediate, non-hydrogen-bonded state. This can be evaluated by calculating the distribution of waiting times for non-hydrogen-bonded OH groups to form a hydrogen bond, which provides the lifetime of OH groups that are not donating a hydrogen bond. If the slower reorientational dynamics is due to jumps that involve an intermediate, non-hydrogen-bonded state, these lifetimes should be longer for the alcohols compared to water. However, it is clear from the distributions, shown in Figure 6, that there is not a significant difference in the waiting-time distributions for all three liquids. Each distribution peaks at short times and decays nearly completely in 1 ps. This demonstrates that the transiently broken hydrogen bonds in the alcohols are no longer lived than those in water.

5. REORIENTATION OF INTACT HYDROGEN BONDS

It is important to note that the hydrogen bond jump times are not the only feature of the reorientational dynamics that changes significantly in the water, methanol, ethanol series. The frame reorientation time, τ_2^{frame}, calculated from the reorientational correlation function for intact hydrogen bonds shown in Figure 7, also slows down between the three liquids as $\tau_2^{frame} \approx 5.6$, 7.3, and 15.5 ps for water, methanol, and ethanol, respectively (see Table 1). These give τ_2 within the EJM, calculated from eq 3, as 2.0, 4.9, and 10.4 ps for water, methanol, and ethanol, in good agreement with the values obtained directly from $C_2(t)$. The trend in τ_2^{frame} may be due to a combination of the liquid viscosity ($\eta = 0.89$, 0.55, and 1.1 Cp for water, methanol, and ethanol, respectively) and the changing effective hydrodynamic volume of the hydrogen-bonded pair; a full understanding will require additional study.

The consequence of the changes in the jump and frame reorientation times is that, in contrast to water, $\tau_2^{frame} < \tau_2^{jump}$
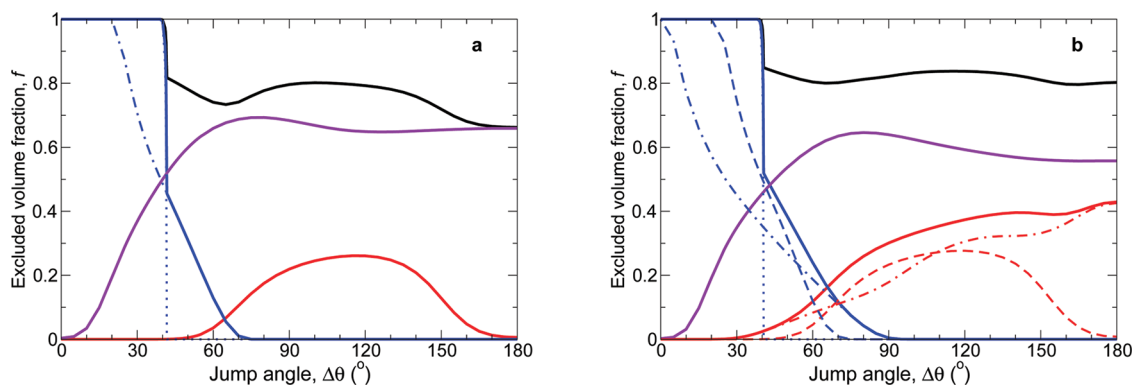
Figure 5. Excluded volume fractions, $f(\Delta\theta)$, (black line) and the individual components due to the hydrogen bond donor (red), acceptor (blue), and all other molecules (violet) are shown for methanol (a) and ethanol (b). The contributions due to the donor CH_2 (dashed red line) and CH_3 (dot-dashed red line) and acceptor O_A (dotted blue line), CH_2 (dashed blue line), and CH_3 (dot-dashed blue line) are also shown.[43]
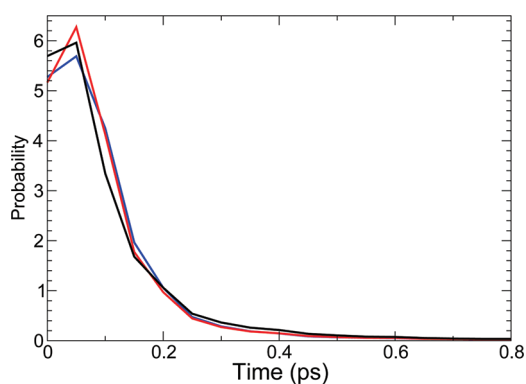

Figure 6. Waiting time distributions for non-hydrogen-bonded OH groups in water (black), methanol (red), and ethanol (blue), obtained using a comparatively strict definition of a hydrogen bond: $R_{OO} \leq 3.1$ Å, $r_{HO} \leq 2.0$ Å, and $\theta_{HOO} \leq 20°$.
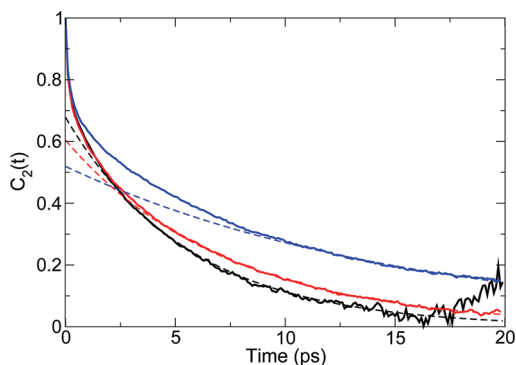

Figure 7. Reorientational correlation function, $C_2(t)$, for intact hydrogen bonds for water (black line), methanol (red line), and ethanol (blue line). The frame reorientation contribution, τ_2^{frame} is obtained from an exponential fit (shown as dashed lines of the same color) over the interval from 5 to 20 ps for water and 10 to 20 ps for methanol and ethanol.

for the alcohols, which implies that the frame reorientation of the intact hydrogen bond becomes the dominant reorientation pathway compared to the hydrogen-bond jumps. This greater importance for the frame reorientation time, which changes

more slowly from water to methanol to ethanol than the jump time, explains why the slowdown in τ_2 is not as large as that for the jump times. In addition, since the reorientation of intact hydrogen bonds is diffusive in nature, it would be expected that the OH reorientation in the alcohols should be better described by a rotational diffusion model. A key prediction of this model is $\tau_n = [n(n+1)D_R]^{-1}$ such that $\tau_1/\tau_2 = 3$ and $\tau_1/\tau_3 = 6$. These relationships are not observed for water ($\tau_1/\tau_2 = 2.0 \pm 0.4$, $\tau_1/\tau_3 = 2.9 \pm 0.6$), but better agreement is found for methanol ($\tau_1/\tau_2 = 2.5 \pm 0.2$, $\tau_1/\tau_3 = 4.6 \pm 0.3$) and, more so, ethanol ($\tau_1/\tau_2 = 3.1 \pm 0.5$, $\tau_1/\tau_3 = 6.5 \pm 1.0$). This is a result of the increasing weight of the frame reorientation time as the jump times are lengthened.

6. SUMMARY

The slower OH-bond reorientational dynamics in methanol and ethanol compared to water can be explained within the extended jump model originally developed for water.[37] The central place of hydrogen-bond switching in the mechanism for reorientation is found to persist. The key factor leading to the slowdown is the volume of the alkyl groups which excludes potential new hydrogen-bonding partners leading to a greater importance for the reorientation time of intact hydrogen bonds, which also slows from water to methanol to ethanol. Whether this mechanistic picture also describes OH reorientation in the higher alcohols is still an open question that is currently under investigation.

7. SIMULATION METHODOLOGY

Classical molecular dynamics (MD) simulations were carried out using the DL_POLY_2 software.[44] Liquid water, methanol, and ethanol were simulated using 343, 385, and 264 molecules, respectively in cubic boxes of side-length 21.725311, 30, and 30 Å, respectively, giving densities of $\rho = 1.00$, 0.759, and 0.748 g/cm^3, respectively. The SPC/E model[45] was used to describe the water interactions while the OPLS-UA force-field[46,47] was used for methanol and ethanol. Lennard-Jones interactions were evaluated with a cutoff of 10.5 Å for water and 15 Å for the alcohols. Long-range electrostatic interactions were included using three-dimensional periodic boundary conditions with a Ewald summation using an Ewald parameter of $\alpha = 0.25$, a $10 \times 10 \times 10$ k-point grid for fast Fourier transforms, and a cutoff of 10.5 (water) or 15 Å (methanol and ethanol).

12177

dx.doi.org/10.1021/jp206875k |J. Phys. Chem. B 2011, 115, 12173–12178

Simulations were initiated from a simple cubic lattice, and equilibrated for 0.5 ns followed by data collection stages of varying lengths. A 1 fs time step was used in all cases and configurations were saved every 8 fs after equilibration. A Nosé–Hoover thermostat[48,49] with a time constant of 1 ps was used to maintain the temperature. Comparison with NVE simulations showed no significant effect on the correlation functions due to the thermostatting. At 298 K, the data collection stage was 2 ns for water and methanol and 10 ns for ethanol. In calculating results at other temperatures (280, 320, 340, and 360 K), 4 ns trajectories were used for ethanol, a 5 ns trajectory for methanol at 280 K data, and 1 ns trajectories for water and methanol for $T \geq 320$ K. Error bars were calculated using block-averaging with 10 blocks and reported at a 95% confidence level using the Student t distribution.[50]

■ AUTHOR INFORMATION

Corresponding Author

*E-mail: wthompson@ku.edu.

Present Addresses

§Department of Chemistry, Emporia State University, Emporia, KS 66801.

■ REFERENCES

(1) Ludwig, R.; Gill, D. S.; Zeidler, M. D. *Z. Naturforsch. A* **1991**, *46*, 89–94.

(2) Ludwig, R.; Rusbuldt, C.; Bopp, P. A.; Zeidler, M. D. *Z. Naturforsch. A* **1995**, *50*, 211–216.

(3) Ludwig, R.; Zeidler, M. D.; Farrar, T. C. *Z. Phys. Chem.* **1995**, *189*, 19–27.

(4) Ludwig, R.; Zeidler, M. D. *Mol. Phys.* **1994**, *82*, 313–323.

(5) Horng, M.; Gardecki, J.; Maroncelli, M. *J. Phys. Chem. A* **1997**, *101*, 1030–1047.

(6) Ferris, T. D.; Farrar, T. C. *Mol. Phys.* **2002**, *100*, 303–309.

(7) Hassion, F. X.; Cole, R. H. *J. Chem. Phys.* **1955**, *23*, 1756–1761.

(8) Denney, D. J.; Cole, R. H. *J. Chem. Phys.* **1955**, *23*, 1767–1772.

(9) O'Reilly, D. E.; Peterson, E. M. *J. Chem. Phys.* **1971**, *55*, 2155–2163.

(10) Asahi, N.; Nakamura, Y. *J. Chem. Phys.* **1998**, *109*, 9879–9887.

(11) Benmore, C. J.; Loh, Y. L. *J. Chem. Phys.* **2000**, *112*, 5877–5883.

(12) Weitkamp, T.; Neuefeind, J.; Fischer, H. E.; Zeidler, M. D. *Mol. Phys.* **2000**, *98*, 125–134.

(13) Wendt, M. A.; Zeidler, M. D.; Farrar, T. C. *Mol. Phys.* **1999**, *97*, 753–756.

(14) Ferris, T. D.; Zeidler, M. D.; Farrar, T. C. *Mol. Phys.* **2000**, *98*, 737–744.

(15) Yamaguchi, T.; Matubayasi, N.; Nakahara, M. *J. Phys. Chem. A* **2004**, *108*, 1319–1324.

(16) Tsukahara, T.; Harada, M.; Tomiyasu, H.; Ikeda, Y. *J. Phys. Chem. A* **2008**, *112*, 9657–9664.

(17) Haughney, M.; Ferrario, M.; McDonald, I. R. *J. Phys. Chem.* **1987**, *91*, 4934–4940.

(18) Pálinkás, G.; Hawlicka, E.; Heinzinger, K. *J. Phys. Chem.* **1987**, *91*, 4334–4341.

(19) Matsumoto, M.; Gubbins, K. E. *J. Chem. Phys.* **1990**, *93*, 1981–1994.

(20) Ferrario, M.; Haughney, M.; McDonald, I. R.; Klein, M. L. *J. Chem. Phys.* **1990**, *93*, 5156–5166.

(21) Sindzingre, P.; Klein, M. L. *J. Chem. Phys.* **1992**, *96*, 4681–4692.

(22) Guàrdia, E.; Sesé, G.; Padró, J. A. *J. Mol. Liq.* **1994**, *62*, 1–16.

(23) van Leeuwen, M. E.; Smit, B. *J. Phys. Chem.* **1995**, *99*, 1831–1833.

(24) Kumar, P. V.; Maroncelli, M. *J. Chem. Phys.* **1995**, *103*, 3038–3060.

(25) Veldhuizen, R.; de Leeuw, S. W. *J. Chem. Phys.* **1996**, *105*, 2828–2836.

(26) Saiz, L.; Pádro, J. A.; Guàrdia, E. *J. Phys. Chem. B* **1997**, *101*, 78–86.

(27) Guàrdia, E.; Martí, J.; Pádro, J. A.; Saiz, L.; Komolkin, A. V. *J. Mol. Liq.* **2002**, *96–7*, 3–17.

(28) Kosztolanyi, T.; Bako, I.; Palinkas, G. *J. Chem. Phys.* **2003**, *118*, 4546–4555.

(29) Wensink, E. J. W.; Hoffmann, A. C.; van Maaren, P. J.; van der Spoel, D. *J. Chem. Phys.* **2003**, *119*, 7308–7317.

(30) Guevara-Carrion, G.; Nieto-Draghi, C.; Vrabec, J.; Hasse, H. *J. Phys. Chem. B* **2008**, *112*, 16664–16674.

(31) Zasetsky, A. Y.; Petelina, S. V.; Lyashchenko, A. K.; Lileev, A. S. *J. Chem. Phys.* **2010**, *133*, 134502.

(32) We note that we have examined other models for methanol and ethanol, including one previously reported to give longer reorientation times for methanol.[17] In all cases, we found equivalent or shorter reorientation times with these other models compared to the OPLS force field used here. Thus, the quantitative discrepancies between the simulations and experimental results still need to be resolved.

(33) Smith, D. W. G.; Powles, J. G. *Mol. Phys.* **1966**, *10*, 451–463.

(34) Lankhorst, D.; Schriever, J.; Leyte, J. C. *Ber. Bunsen. Phys. Chem.* **1982**, *86*, 215–221.

(35) Ludwig, R.; Weinhold, F.; Farrar, T. C. *J. Chem. Phys.* **1995**, *103*, 6941–6950.

(36) Laage, D.; Hynes, J. T. *Science* **2006**, *311*, 832–835.

(37) Laage, D.; Hynes, J. T. *J. Phys. Chem. B* **2008**, *112*, 14230–14242.

(38) Laage, D.; Stirnemann, G.; Hynes, J. T. *J. Phys. Chem. B* **2009**, *113*, 2428–2435.

(39) The distribution of jump angles is best obtained by identifying the transition states for hydrogen bond exchanges.[37] However, a relatively simple alternative is to calculate the $O_A–O_D–O_B$ angle immediately after the jump, that is, at the first time step after which the $O_D–H\cdots O_B$ hydrogen bond has been formed. This approach is used in this work and we have verified it is an accurate alternative by comparison to preliminary calculations based on identification of the jump transition state structures.

(40) An NVE ensemble and experimental, temperature-dependent densities were used in ref 37.

(41) Stirnemann, G.; Sterpone, F.; Laage, D. *J. Phys. Chem. B* **2011**, *115*, 3254–3262.

(42) The calculated slowdown factors are approximate as a fixed value of $R^{\ddagger}$, taken from previous work on water,[38] is assumed at all jump angles for both methanol and ethanol.

(43) Note that the excluded volume contributions are not additive as some locations are simultaneously excluded by multiple sites.

(44) The DL_POLY Molecular Simulation Package. http://www.ccp5.ac.uk/DL_POLY (accessed April 15, 2009).

(45) Berendsen, H. J. C.; Grigera, J. R.; Straatsma, T. P. *J. Phys. Chem.* **1987**, *91*, 6269–6271.

(46) Jorgensen, W. L. *J. Phys. Chem.* **1986**, *90*, 1276–1284.

(47) Jorgensen, W. L.; Madura, J. D.; Swenson, C. J. *J. Am. Chem. Soc.* **1984**, *106*, 6638–6646.

(48) Nosé, S. *Mol. Phys.* **1984**, *52*, 255–268.

(49) Hoover, W. G. *Phys. Rev. A* **1985**, *31*, 1695–1697.

(50) Shoemaker, D. P.; Garland, C. W.; Nibler, J. W. *Experiments in Physical Chemistry*; McGraw-Hill: New York, 1989.

12178

dx.doi.org/10.1021/jp206875k |*J. Phys. Chem. B* 2011, 115, 12173–12178